

## Why Have Continuum Theories Previously Failed to Describe Sandpile Formation?

Qijun Zheng and Aibing Yu\*

*Laboratory for Simulation and Modeling of Particulate Systems, School of Materials Science and Engineering,  
The University of New South Wales, Sydney, New South Wales 2052, Australia*

(Received 1 November 2013; revised manuscript received 1 December 2013; published 5 August 2014)

Granular piling may or may not induce a counterintuitive phenomenon of pressure dip at the center of a pile base. Understanding the behavior is a long-standing challenge in granular dynamics modeling. Here we show that the experimental observations of dip or nondip piles can be satisfactorily reproduced by the classic elastoplastic models. Our results demonstrate that (i) dynamic history is a critical factor in the successful description of a piling process and (ii) the dip phenomena are complicated, involving numerous variables associated not only with piling operation but also material properties. Our findings can explain why previous attempts failed to describe piling processes and may open up a new direction to describe granular materials in nature and many industrial processes.

DOI: 10.1103/PhysRevLett.113.068001

PACS numbers: 45.70.Cc, 47.57.Gc, 83.80.Fg

Granular material, as the second largest material (next to water) we humans handle, can widely be found in nature and in industry [1,2]. However, different from its comparative phases such as gas and liquid, it still lacks a general theory to describe its dynamics. Elastoplastic theory is one of the theories proposed for this purpose [3]. But it has been challenged by recent observations of force transmission in granular beds [4–11], particularly because of its “failure” to predict the stress dip beneath a pile [4,5,7,9]. It is a very intriguing phenomenon that the stress is not maximum but locally minimum below the pile apex. As noted by de Gennes [6], this phenomenon is directly related to the physics of granular matter, which in 1998 was at the level of solid-state physics in the 1930s and needs intensive studies for many years. Clearly, breakthrough research is much needed to overcome this problem, particularly in the formulation of governing equations and associated constitutive relations for granular materials.

The traditional elastoplastic models are commonly thought ineffective in solving the dip problem [12]. Thus new constitutive relations such as the hyperbolic equations [10,11,13–16] and the anisotropic elasticity [12,17,18] have been developed to overcome this problem. Nevertheless, it seems none of them can be used generally, because they cannot realistically mimic the piling processes that may or may not produce a stress dip beneath a pile of particles. Indeed, recent experimental studies have shown that granular piling is a very complicated process, and the presence of a dip strongly depends on the construction or growth method of the pile. For example, it is reported that in a pile produced by depositing particles through a localized source, the pressure right below the pile apex is not the maximum but shows a local decrease or “dip” [4,5,7]. On the other hand, a pile prepared by a rainfall-like deposition will have no observable dip [7]. This indicates that in the analysis of a pile, the construction history matters.

One important issue then arises: what will the results be if we indeed follow the experimental procedures to prepare a pile in modeling and simulation? This issue represents a critical test of the applicability of a theory in describing granular materials. We here carry out such a test based on two classic elastoplastic models: the Mohr-Coulomb (MCEP) and Drucker-Prager (DPEP) [3,19]. We will show that either of the two models, after being coupled with the dynamic history, can satisfactorily reproduce the experimental observations of dip or nondip piles. The results can also explain why the previous continuum theories fail in describing the formation of a sandpile.

Figure 1 illustrates how the conical piles are constructed in our numerical tests similar to the physical experiments [7]. The procedures are as follows. First, a packing of particles is formed in the hopper. The particles are then discharged from the hopper under gravity and piled up on a plate below the hopper. This piling process is continuous until the desired pile radius  $R$  is achieved. Finally, some additional period is used for the pile to reach its static state (monitored in terms of the total kinetic energy of the system). The process inevitably involves a large flowage or plastic deformation of material which is irreversible and history dependent. Consequently, different construction methods will generate different plastic deformations and hence different piling behaviors.

In this work, granular material is treated as a continuum medium assuming that the system scale is always much greater than component particles or grains. Its dynamics is governed by conservation equations of mass, momentum, and energy, with a constitutive model describing its intrinsic characteristics. To take the dynamic history into account, an advanced numerical technique—Eulerian-formulation finite element analysis (FEA)—is employed in this study. This Eulerian approach is essentially a “Lagrange-plus-remap” process. In each calculation step,

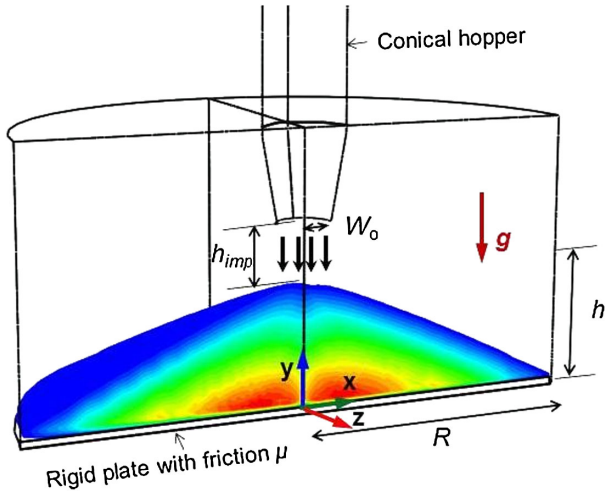


FIG. 1 (color online). Construction methods of conical piles. Half cone is shown with  $XY$  plane being the cross section.  $R$  and  $h$  are the base radius and height of the final pile, respectively, controlled by the dimension of plate because excess material from the hopper will avalanche down the plate automatically.  $W_o$  is the radius of hopper orifice. If  $R$  is much larger than  $W_o$ , the procedure corresponds to the localized source piling method; if  $R/W_o \approx 1$ , the procedure is close to the rainfall-like piling method in experiment [7]. The falling height,  $h_{imp}$ , is preserved during the pile growth by slowly lifting the hopper. The construction procedures are similar for rectangular wedge-shaped piles.

it first accounts for the deformation of mesh (attached to material) similarly to the conventional Lagrangian FEA, and then remaps the obtained results of field variables back to the original mesh using a second-order convection algorithm. Thereby the original mesh can be preserved throughout the simulation duration, and granular material flows through the grids like a fluid. An enhanced immersed boundary method [19] is used to consider the contact between the Eulerian material and the boundaries such as the support plate and hopper wall. Moreover, to determine the volume of granular material in the computational mesh, a variable Eulerian volume fraction (EVF) is defined, which equals unity for grids full of material and zero for void grids [19].

The elastoplastic models considered, i.e., MCEP and DPEP, have both been well documented in the literature, each comprising an elastic law, a yield criterion, and a rule of plastic flow [3,19]. For details, please refer to the Supplemental Material [20]. The two models can describe the dual solid- and fluid-like behaviors: below the yield criterion, material represented by a model behaves like an elastic solid; otherwise, it flows like a fluid. The major difference between them lies in the yield criterion: MCEP can be represented by a conical-prism shaped surface in three-dimensional stress space while DPEP corresponds to a smoother regular-cone surface. As a result, to achieve the same angle of repose for the pile, different values of internal

friction angle  $\varphi$  need to be used for the two models. In this Letter, unless otherwise specified, we select  $\varphi = 30^\circ$  for the MCEP model and  $\varphi = 45^\circ$  for the DPEP model, so that they can produce approximately the same angle of repose for conical piles. The rests of the two models are similar, both using isotropic elasticity and nonassociated flow rule. Other material parameters used are given in Fig. 2.

Figure 2 demonstrates the profile of pressure  $\sigma_{yy}$  (normal stress in the  $y$  direction) across the bottom of a pile. The pressure is normalized by the hydrostatic pressure as  $\sigma_{yy}/\rho gh$  and the  $z$  coordinate is normalized by the pile radius as  $z/R$ . Obviously, the FEA produces distinct pressure dips in the case of  $R/W_o = 10$  (localized source history), and a little dip in the case of  $R/W_o = 1$  (rainfall-like history). The FEA predicts a greater dip in conical piles than in wedge-shaped piles if other conditions are the same. All the predictions are comparable to the observations [7]. Note that here we simply take typical properties of granular materials (sand and glass beads) with no fitting exercise. As will be discussed, these parameters may affect the results and their tuning can improve the agreement.

The dip or nondip behavior is therefore very much related to the piling history. To depict the mechanism,

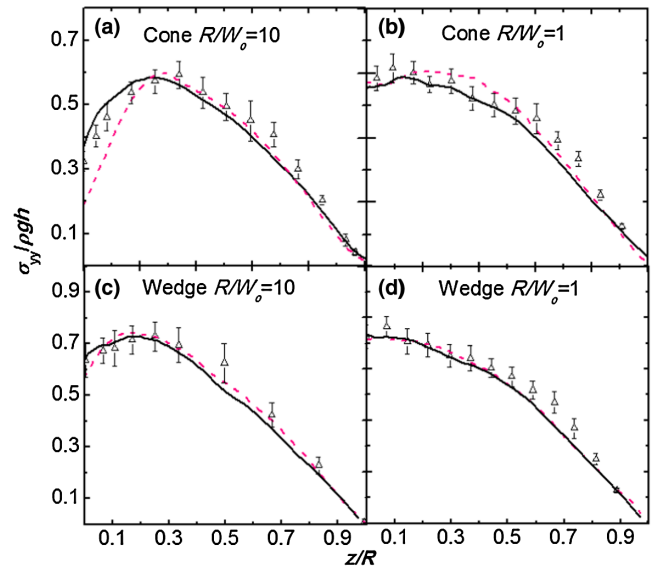


FIG. 2 (color online). Profiles of the normalized pressure  $\sigma_{yy}/\rho gh$  for four different piles: (a) conical pile produced with  $R/W_o = 10$ , (b) conical pile produced with  $R/W_o = 1$ , (c) rectangular wedge-shaped pile with  $R/W_o = 10$ , and (d) rectangular wedge-shaped pile with  $R/W_o = 1$ . Points (open triangle) denote the experimental results while solid and dash lines show the predictions by the MCEP model and DPEP model respectively. The operational and material parameters used in the present FEA simulation are: Young's modulus  $E/\rho g W_o = 1276$ , where  $\rho$  is the bulk density of material and  $g$  the acceleration, falling height  $h_{imp}/W_o = 0$  and Poisson's ratio  $\nu = 0.3$ . The internal friction angle  $\varphi = 30^\circ$  for the MCEP model and  $\varphi = 45^\circ$  for the DPEP model. Cohesion  $c$  and angle of dilatancy  $\psi$  are set to zero. The friction between granular matter and floor is taken as  $\mu = 0.3$ .

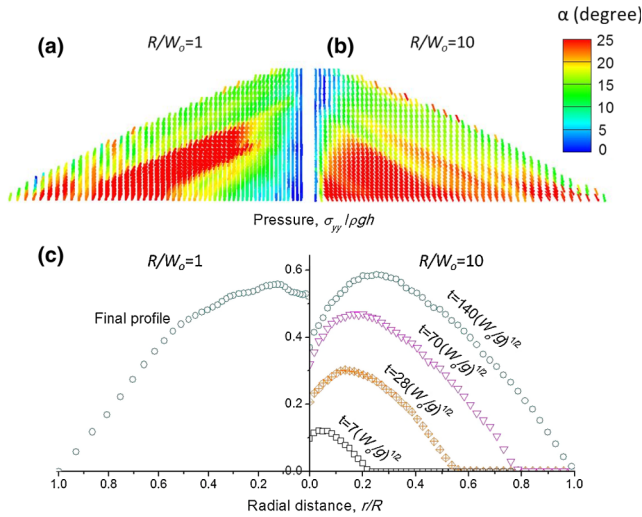


FIG. 3 (color online). The angle of PAS,  $\alpha$  (degree), for different piling histories: (a) rainfall deposit ( $R/W_o = 1$ ), (b) localized source deposit ( $R/W_o = 10$ ), and (c) temporal pressure profiles at the pile base (right side). For the rainfall deposit, only the final pressure profile is presented (left side) because the shape of a pile does not form until the last stage. Here  $\alpha$  is calculated based on the three in-plane stress components:  $\sigma_{xx}$ ,  $\sigma_{yy}$  and  $\sigma_{xy}$ .

Fig. 3 compares the patterns of principal axes of stress (PAS) between the dip and nondip piles. PAS represents the main path of force transmission analogous to the network of contact forces in discrete particle simulations [25–28]. Parameter  $\alpha$  is used to measure the direction of PAS with respect to the vertical  $y$ -axis in the bulk. The results indicate that in the nondip case ( $R/W_o = 1$ ), the PAS is essentially upright in the core regime (small  $\alpha$ ), but in the dip case, a much larger  $\alpha$  is present. In the latter, the PAS plays a role of “force arching” [14,25,26] by transmitting the self-weight to the outer regime and thereby alleviating the pressure in the core regime. This offers one reason why a pile may or may not have a dip. In the localized source history ( $R/W_o = 10$ ), granular material tends to move laterally over the support plate, particularly under the impact of falling particles at the pile apex and the resulting horizontal shear. Because of the memory effect as discussed in [20], this eventually causes a big  $\alpha$  and forms a dip at the base center. By contrast, for the rainfall deposit method ( $R/W_o < 2$ ), the particles and the impact momentum are more evenly distributed over the support plate, less horizontal shear stress is generated, and hence they are less likely to establish a stress dip in the center.

The mechanism depicted in the current analysis is different from those reported [12,14,18,29], which largely ignore the construction history and can only produce piles always with a stress dip or with no stress dip. In particular, inspired by the picture of force arches, some researchers [14,29] disregarded the concept of material strain and used a local rule that directly correlates the stress components to

close the governing equations. The “fixed principal axes” (FPA) hypothesis [14] is one such rule; it postulates that the PAS everywhere across the pile has a uniform inclination angle. While this hypothesis does generate the desirable pressure distribution in a particular conical heap, our results in Fig. 3 clearly indicate that it is in fact not a necessary condition for the occurrence of stress dips, and inhomogeneous PAS can also be effective. Broadly speaking, the FPA hypothesis is too simplistic to be general and better regarded as a special case of all the possible PAS pictures.

A fundamental feature of the present model is its capability to take into account granular dynamics. Conceptually, the historical effect can be automatically recorded in a simulation via the path-dependent characteristic of plastic deformation. The previous analyses, on the other hand, only consider the final equilibrium or static state of a pile. The historical effect is embodied by acknowledging a few factors in their framework, for example, in the pattern of PAS ( $\alpha$ ) in the hyperbolic equation [14], the stress response function in the anisotropic elasticity theory [18], or the Rankine states (passive or active) in the plastic limit analysis [12]. How to precisely determine those factors in terms of construction history remains a subtle but complex issue, especially considering the large variance between different granular systems (piles, storage hoppers, and rotary drums, to name but a few). In fact, a few FEA simulations [12,30,31] had been carried out on the piling process. The MCEP and DPEP models were shown ineffective in these studies, and in order to generate a stress dip, some complex models which often involve particular constitutive relations or treatments were required. However, our present results demonstrate that the “failure” should be attributed to the ignorance or inaccurate modeling of the piling history in the previous attempts. A comprehensive analysis of the previous approaches against the present one is detailed in Supplemental Material [20].

The dynamic history is related to many factors. Hence, the dip phenomenon should be affected by many variables associated with piling operation and material properties. To test the sensitivity of our FEA results and to investigate the parameter dependency, we carried out some numerical experiments focusing on conical piles using the MCEP model (the DPEP model produces similar results). For convenience, the degree of dip (DOD) is quantified as  $\text{DOD} = 1 - \text{pressure at the center}/\text{the maximum pressure at the pile base}$ . Figure 4 shows the effects of some operational and material parameters on DOD. In the preceding discussion, only two special cases are considered corresponding to the rainfall-like and localized source piling methods respectively. Here a continuous variation of  $R/W_o$  is examined to show that the crossover between dip and nondip occurs at around  $R/W_o = 2$ . Once  $R/W_o > 3$ , the effect of  $R/W_o$  disappears, indicating that a scaling law applies and the pressure profiles with

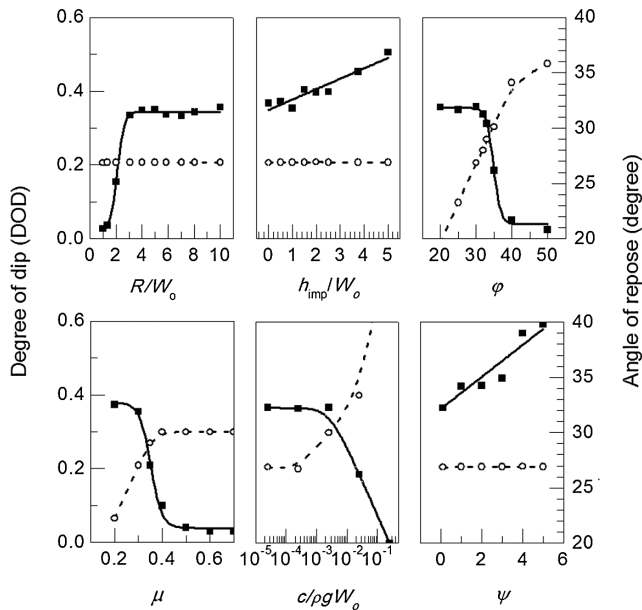


FIG. 4. Dependences of the degree of dip (DOD) (filled square) and angle of repose (open circle) on some piling parameters. The angle of repose is measured based on the profiles of piles using a protractor tool. In each figure, only one parameter is varied while others take the base values given in Fig. 2 and by default,  $R/W_o = 10$ .

different pile sizes  $R$  should collapse into one curve after nondimensionalization as demonstrated in experiments [4,7]. The falling height  $h_{\text{imp}}$  here stands for the kinetic impact in the system. The results show that increasing  $h_{\text{imp}}$  can increase the impact and slightly enhance the pressure dip, which qualitatively agrees with the previous experiment [7].

Material properties also play an important role here. It can be seen that a high value of internal friction angle  $\varphi$ , base friction  $\mu$  or cohesion  $c$  can lead to the disappearance of the pressure dip, even when a localized-source piling method is used. The angle of repose is commonly used as an adverse indicative of flowability in powder technology [26,32,33]. It may to some degree be linked to the dipping mechanism. Figure 4 suggests that the pressure dip is more likely to occur to materials of low angle of repose. In addition, the dip is shown to rise slightly with the increase of material dilatancy  $\psi$ .

It is clear from Fig. 4 that the dipping phenomena are complicated, dependent on many variables related to piling operation and material properties. While more precise tests are necessary in the future in order to better understand the phenomena, the present results add one more reason, in addition to the dynamic history, as to why the previous attempts focusing on one or two variables often fail to be general.

How to develop a general theory to describe granular materials has been a challenge in the research community for many years. It is commonly held that the classical continuum

theories fail, thereby more and more complicated theories have been proposed. However, here we overturn such a trend through a study of a very representative and critical problem, namely the stress dip beneath a sandpile. In particular, we show that the classical elastoplastic theories such as MCEP and DPEP can satisfactorily predict this intriguing phenomenon under various conditions, and the piling history is critical to successful modeling and simulation. Thus, the traditional elastoplastic theories still have a great potential to describe the mechanics of granular materials, although as a continuum theory, they may have limitations in probing the local, particle scale micromechanics [11,27,28,33–35]. This continuum description should be useful for large-scale applications, e.g., the prediction and prevention of natural disasters (e.g., landslide, volcano lava, and other aeromechanical phenomena), design and control of industrial granular processes (e.g., stockpiling, storage silos or hoppers, rotating drums, blast furnaces, and so on). In fact, our recent studies have demonstrated that the proposed approach can successfully describe complicated granular flows, including different flow regimes related to solid- and fluid-like behaviors, in a hopper or rotating drum. Thus, coupling the classical continuum description with dynamic history not only explains why previous attempts fail in describing piling processes but also open up a new direction to describe granular materials in nature and many industrial processes. In the future, it is certainly worthwhile to apply this approach to solve different granular dynamics problems and, at the same time, to identify their application boundaries.

We thank the Australian Research Council for the financial support of this work.

\*Present address: Department of Chemical Engineering, Monash University, Clayton, Victoria 3800, Australia. aibing.yu@monash.edu

- [1] H. M. Jaeger, S. R. Nagel, and R. P. Behringer, *Rev. Mod. Phys.* **68**, 1259 (1996).
- [2] P. Richard, M. Nicodemi, R. Delannay, P. Ribiere, and D. Bideau, *Nat. Mater.* **4**, 121 (2005).
- [3] R. M. Nedderman, *Statics and Kinematics of Granular Materials* (Cambridge University Press, Cambridge, England, 1992).
- [4] J. Smid and J. Novosad, in *Proceedings of the 1981 Powtech Conference* (Institution of Chemical Engineers, Rugby, England, 1981) Vol. 63.
- [5] R. Brockbank, J. M. Huntley, and R. C. Ball, *J. Phys. II (France)* **7**, 1521 (1997), Vol. **63**.
- [6] P. G. de Gennes, *Rev. Mod. Phys.* **71**, S374 (1999).
- [7] L. Vanel, D. Howell, D. Clark, R. P. Behringer, and E. Clément, *Phys. Rev. E* **60**, R5040 (1999).
- [8] M. Da Silva and J. Rajchenbach, *Nature (London)* **406**, 708 (2000).
- [9] J. Geng, E. Longhi, R. P. Behringer, and D. W. Howell, *Phys. Rev. E* **64**, 060301 (2001).

- [10] C. Goldenberg and I. Goldhirsch, *Nature (London)* **435**, 188 (2005).
- [11] S. Luding, *Nature (London)* **435**, 159 (2005).
- [12] S. B. Savage, in *Physics of Dry Granular Media* (Springer, New York, 1998), p. 25.
- [13] J. P. Bouchaud, M. E. Cates, and P. Claudin, *J. Phys. I (France)* **5**, 639 (1995).
- [14] J. P. Wittmer, P. Claudin, M. E. Cates, and J. P. Bouchaud, *Nature (London)* **382**, 336 (1996).
- [15] J. P. Wittmer, M. E. Cates, and P. Claudin, *J. Phys. I (France)* **7**, 39 (1997).
- [16] M. E. Cates, J. P. Wittmer, J. P. Bouchaud, and P. Claudin, *Philos. Trans. R. Soc. London, A* **356**, 2535 (1998).
- [17] C. Gay and R. A. d. Silveira, *Europhys. Lett.* **68**, 51 (2004).
- [18] A. P. F. Atman, P. Brunet, J. Geng, G. Reydellet, P. Claudin, R. P. Behringer, and E. Clement, *Eur. Phys. J. E* **17**, 93 (2005).
- [19] Abaqus 6.10 Analysis User Manual (Dassault Systèmes Simulia Corp, Providence, RI).
- [20] See Supplemental Material at <http://link.aps.org/supplemental/10.1103/PhysRevLett.113.068001> for details, which also refers to the works [21–24].
- [21] S. Okazawa, K. Kashiwara, and Y. Kaneko, *Int. J. Numer. Methods Eng.* **72**, 1544 (2007); D. J. Benson and S. Okazawa, *Comput. Methods Appl. Mech. Eng.* **193**, 4277 (2004); D. J. Benson, *Comput. Mech.* **15**, 558 (1995).
- [22] P. Jop, Y. I. Forterre, and O. Pouliquen, *Nature (London)* **441**, 727 (2006).
- [23] Y. M. Jiang and M. Liu, *Phys. Rev. Lett.* **91**, 144301 (2003); K. Kamrin and G. Koval, *Phys. Rev. Lett.* **108**, 178301 (2012); D. L. Henann and K. Kamrin, *Proc. Natl. Acad. Sci. U.S.A.* **110**, 6730 (2013); S. Sarkar, D. Bi, J. Zhang, R. P. Behringer, and B. Chakraborty, *Phys. Rev. Lett.* **111**, 068301 (2013); N. Gland, P. Wang, and H. A. Makse, *Eur. Phys. J. E* **20**, 179 (2006); H. A. Makse, N. Gland, D. L. Johnson, and L. Schwartz, *Phys. Rev. E* **70**, 061302 (2004).
- [24] K. Kamrin, *Int. J. Plast.* **26**, 167 (2010).
- [25] See, for example, S. Luding, *Phys. Rev. E* **55**, 4720 (1997); G. Oron and H. J. Herrmann, *Phys. Rev. E* **58**, 2079 (1998); K. Liffman, D. Y. C. Chan, and B. D. Hughes, *Powder Technol.* **72**, 255 (1992); **78**, 263 (1994); H. G. Matuttis, *Granular Matter* **1**, 83 (1998); H. G. Matuttis and A. Schinner, *Granular Matter* **1**, 195 (1999).
- [26] Y. C. Zhou, B. H. Xu, A. B. Yu, and P. Zulli, *Powder Technol.* **125**, 45 (2002).
- [27] H. P. Zhu, Z. Y. Zhou, R. Y. Yang, and A. B. Yu, *Chem. Eng. Sci.* **62**, 3378 (2007).
- [28] H. P. Zhu, Z. Y. Zhou, R. Y. Yang, and A. B. Yu, *Chem. Eng. Sci.* **63**, 5728 (2008).
- [29] S. F. Edwards and C. C. Mounfield, *Physica A (Amsterdam)* **226**, 25 (1996).
- [30] J. Tejchman and W. Wu, *Granular Matter* **10**, 399 (2008).
- [31] J. Ai, J. Chen, J. Rotter, and J. Ooi, *Granular Matter* **13**, 133 (2011).
- [32] D. McGlinchey, *Bulk Solids Handling: Equipment Selection and Operation* (Blackwell, Birmingham, AL, 2008).
- [33] N. Topić, J. A. C. Gallas, and T. Pöschel, *Phys. Rev. Lett.* **109**, 128001 (2012).
- [34] M. R. Shaebani, M. Madadi, S. Luding, and D. E. Wolf, *Phys. Rev. E* **85**, 011301 (2012).
- [35] A. H. Clark, L. Kondic, and R. P. Behringer, *Phys. Rev. Lett.* **109**, 238302 (2012).